JOURNAL OF GUIDANCE, CONTROL, AND DYNAMICS
Vol. 24, No. 3, May–June 2001

Improved Deployment Characteristics of a Tether-Connected Munition System

Geoffrey Frost* and Mark Costello†
Oregon State University, Corvallis, Oregon 97331

This study investigates the effect of a tether reel resistance mechanism intended to improve the unreeling process of a tether line connected to two projectiles comprising a munition system. The munition system considered is released from an aircraft at altitude and falls toward a target on the ground. Reel resistance models, based on feasible mechanisms, are generated as functions of drop speed, projectile mass, drag coefficient ratio, and tether line stiffness. Reel configurations are determined to decrease tether line loads, maximum acceleration on the follower projectile, time to reach a steady-state condition, and terminal miss distance. Reel resistance based on either the tether line pay out or the tether pay out rate provides a powerful means to improve system performance. Resistance as a function of tether line pay out yields the overall best performance; however, resistance based on tether line pay out rate provides suitable performance over a wider band of drop speeds, mass ratios, and drag coefficient ratios.

Nomenclature

A_n	=	projected area of the follower object
A_{w_i}	=	wetted area of the ith element
C_{D_n}	=	coefficient of drag for the follower object
C_{fp}	=	coefficient of the flat-plate drag
C_{sf}	=	coefficient of the skin-friction drag
c_i	=	damping coefficient for the ith element
F_r	=	resistance force of the reel
F_{T_j}	=	magnitude of the elastic line force for the jth element
I_r	=	mass moment of inertia for the reel
i	=	bead index
j	=	line element index
k_i	=	stiffness coefficient for the ith element
l_i	=	unstretched length of the ith element
m_j	=	mass of the jth bead
ml	=	tether line mass per unit length
m_r	=	mass of the reel
n	=	number of the follower object
r	=	effective radius of the tether reel
r_i	=	directional vector of the ith element
s	=	total length of tether line unspooled from the tether reel
$\dot{s}$	=	speed of the tether line exiting the tether reel
$\ddot{s}$	=	acceleration of the tether line exiting the tether reel
$V_{\text{fp}_{j,0}}$	=	magnitude of velocity of the jth bead normal to ith $-$ 1 tether element
$V_{\text{fp}_{j,1}}$	=	magnitude of velocity of the jth bead normal to ith tether element
$V_{\text{sf}_{j,0}}$	=	component of velocity of the jth bead parallel to ith $-$ 1 tether element
$V_{\text{sf}_{j,1}}$	=	component of velocity of the jth bead parallel to ith tether element
W_j	=	weight of the jth bead
$X_{D_J}, Y_{D_J}, Z_{D_J}$	=	drag force of the jth bead in the inertial reference frame
$X_{T_i}, Y_{T_i}, Z_{T_i}$	=	elastic line force of the ith element in the inertial reference frame
x_j, y_j, z_j	=	position vector components of the jth bead in the inertial reference frame
Δl_i	=	distance between each node for the ith element
Δv_i	=	magnitude of the velocity difference between each node for the ith element
$\Delta x_j, \Delta y_j, \Delta z_j$	=	position difference between each node for the jth element in the inertial reference frame
ρ_j	=	air density at the altitude of each bead

Received 20 December 1999; revision received 28 May 2000; accepted for publication 20 July 2000.

*Graduate Research Assistant, Department of Mechanical Engineering.
†Assistant Professor, Department of Mechanical Engineering.

Introduction

WHEREAS the use of tethers in aerospace vehicles is by no means new,[1–5] it has historically not been employed in weapon systems. Some new weapon systems utilize two projectiles connected by a tether line,[6,7] where the lead projectile is a munition and the follower projectile is a sensor platform. The weapon is released from an aircraft and falls toward a target. Both projectiles are initially rigidly attached and separate at a prespecified time after release from the parent aircraft. Subsequently, the tether line begins to unreel. Maximum tether line loads occur shortly after the tether is fully deployed, and this point is called the snatch point. Snatch loads are typically large, to the point where line failure is an important concern. Designers must balance the need to unreel the tether line in a specified period of time while at the same time limiting line loads and follower projectile acceleration. After the tether line is completely payed out and vibration from the snatch point subside, the munition system approaches a steady state as the projectiles and tether line approach the target. A schematic of the various flight phases for the weapon system concept is shown in Fig. 1.

The work presented here considers the use of two types of reel resistance mechanisms, namely, reel resistance proportioned to the length of line unspooled from the reel (LLM) and reel resistance proportional to the rate at which line unspools from the reel (LRM). The LLM device can be realized by mounting the reel on a threaded shaft such that when the reel unspools, it displaces along the reel axis of symmetry. A helical compression spring connected to the reel and casing provides a resistant moment linearly related to the length of line released from the reel. The LRM mechanism can be realized with a centrifugal clutch. For both devices, resistance parameters are selected by minimizing an objective function containing pertinent performance characteristics. Performance characteristics such as tether line loads, projectile acceleration, miss distance, and time for the system to reach steady state are estimated using a nonlinear flight dynamic model.

Munition System Dynamic Model

As shown in Fig. 2, the weapon system is modeled as a series of particles connected by a spring and damper in parallel. The lead and follower projectiles are assumed to be aerodynamically stable and are modeled as point masses with three translational degrees of freedom. Likewise, each tether bead is modeled as a point mass, also with three translational degrees of freedom. Gravitational, aerodynamic,

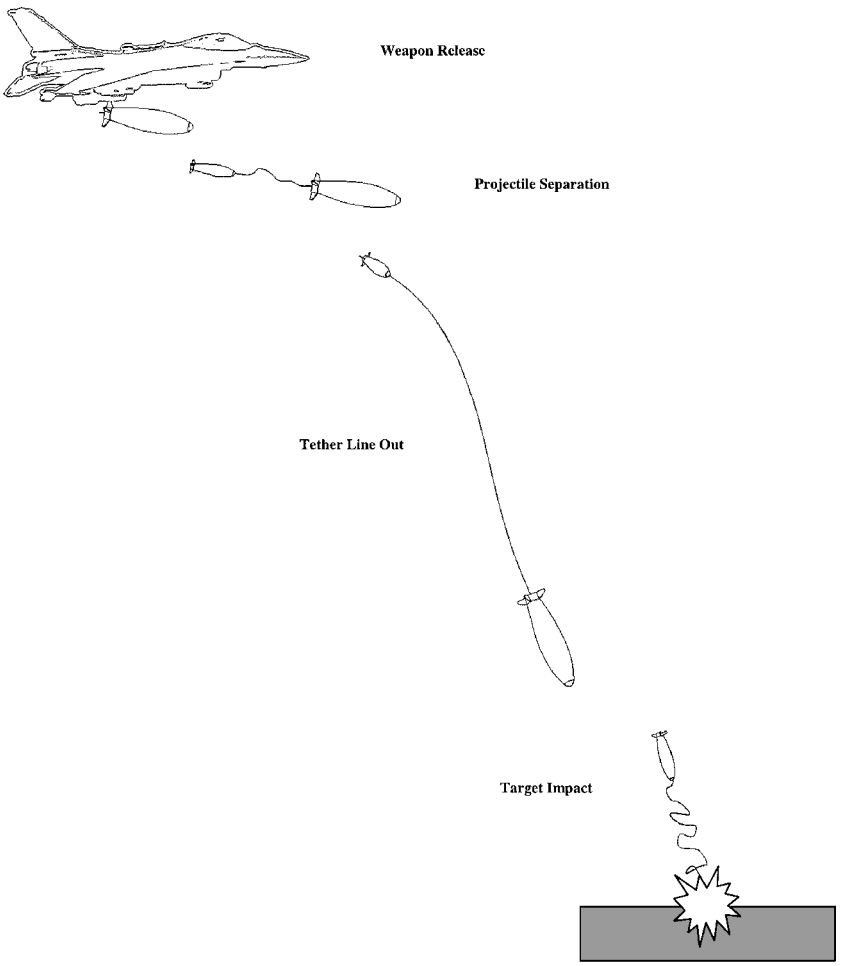

Fig. 1 Flight phases for weapon system concept.

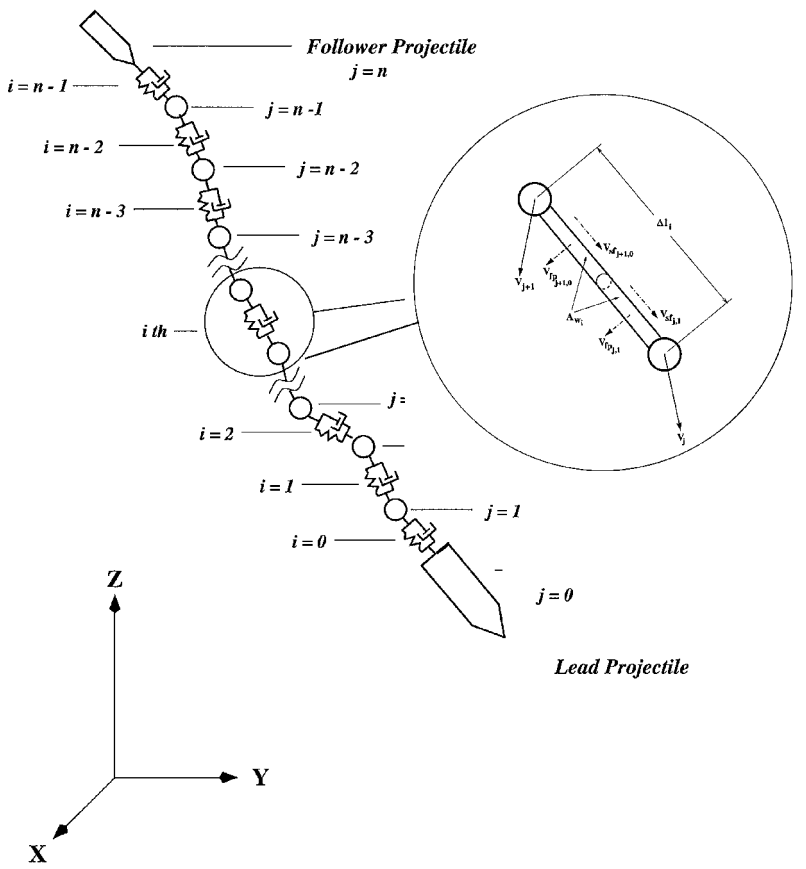

Fig. 2 Dynamic model diagram.

and elastic forces act on both projectiles and the tether beads. The lead and follower objects are designated as the 0th and nth nodes, respectively. The tether is split into $n-1$ particles, or beads, designated by j, and n tether line elements designated with i. The Earth's surface is used as an inertial reference frame. Air density is computed using a standard atmosphere model.[8]

When the tether is fully deployed, the equations of motion for the follower projectile n and the jth tether bead are given by

$$m_n \begin{Bmatrix} \ddot{x} \\ \ddot{y} \\ \ddot{z} \end{Bmatrix}_n = \begin{Bmatrix} X_D \\ Y_D \\ Z_D \end{Bmatrix}_n - \begin{Bmatrix} X_T \\ Y_T \\ Z_T \end{Bmatrix}_{n-1} + \begin{Bmatrix} 0 \\ 0 \\ W \end{Bmatrix}_n \tag{1}$$

$$m_j \begin{Bmatrix} \ddot{x} \\ \ddot{y} \\ \ddot{z} \end{Bmatrix}_j = \begin{Bmatrix} X_T \\ Y_T \\ Z_T \end{Bmatrix}_{i+1} - \begin{Bmatrix} X_T \\ Y_T \\ Z_T \end{Bmatrix}_i + \begin{Bmatrix} X_D \\ Y_D \\ Z_D \end{Bmatrix}_j + \begin{Bmatrix} 0 \\ 0 \\ W_T \end{Bmatrix}_j \tag{2}$$

The lead projectile (0) equations are identical in form to Eq. (1). The elastic forces are due to the spring and damping characteristics of the tether. These forces are always parallel to the direction of the line. The magnitudes of the tether forces are

$$F_{T_i} = \begin{bmatrix} F_{T_0} & F_{T_1} & \cdots & F_{T_{n-1}} \end{bmatrix} \tag{3}$$

$$F_{T_i} = \begin{Bmatrix} k_i(\Delta l_i - l_i) + c_i \Delta v_i, & \Delta l_i \geq l_i \\ 0, & \Delta l_i < l_i \end{Bmatrix} \tag{4}$$

The elastic tether forces expressed in inertial coordinates are

$$\begin{Bmatrix} X_T \\ Y_T \\ Z_T \end{Bmatrix}_i = \frac{F_{T_i}}{\Delta l_i} \begin{Bmatrix} \Delta x_i \\ \Delta y_i \\ \Delta z_i \end{Bmatrix} \tag{5}$$

The tether line forces exerted on adjacent particles are equal in magnitude and opposite in direction.

The follower projectile drag force is

$$\begin{Bmatrix} X_D \\ Y_D \\ Z_D \end{Bmatrix}_n = -\frac{1}{2}\rho_n \sqrt{\dot{x}_n^2 + \dot{y}_n^2 + \dot{z}_n^2} A_n C_{D_n} \begin{Bmatrix} \dot{x} \\ \dot{y} \\ \dot{z} \end{Bmatrix}_n \tag{6}$$

The projectile drag coefficients are Mach number dependent and are computed by linear interpolation of tabulated data. The particle projectile model used in this study is suitable for analysis of gross projectile motion; however, more sophisticated six-degree-of-freedom projectile dynamic models are available.[9]

The aerodynamic force on the tether line includes skin-friction drag along the tether line and flat plate drag perpendicular to the tether line (personal communication from S. Djerassi, 1997). To determine the tether drag, it is useful to define a unit vector whose measure numbers are given by

$$\begin{Bmatrix} r_x \\ r_y \\ r_z \end{Bmatrix}_i = \frac{1}{\Delta l_i} \begin{Bmatrix} \Delta x_i \\ \Delta y_i \\ \Delta z_i \end{Bmatrix} \tag{7}$$

The skin-friction and flat-plate drag for each element are given by

$$D_{\mathrm{sf}_{j,0}} = -\tfrac{1}{2}\rho_j A_{w_{i-1}} C_{\mathrm{sf}} V_{\mathrm{sf}_{j,0}} \left| V_{\mathrm{sf}_{j,0}} \right| \tag{8}$$

$$D_{\mathrm{fp}_{j,0}} = -\tfrac{1}{2}\rho_j A_{w_{i-1}} C_{\mathrm{fp}} \left(V_{\mathrm{fp}_{j,0}} \right)^2 \tag{9}$$

The tether bead aerodynamic forces expressed in the inertial frame are

$$\begin{Bmatrix} X_D \\ Y_D \\ Z_D \end{Bmatrix}_j = D_{\mathrm{sf}_{j,1}} \begin{Bmatrix} r_x \\ r_y \\ r_z \end{Bmatrix}_i + D_{\mathrm{sf}_{j,0}} \begin{Bmatrix} r_x \\ r_y \\ r_z \end{Bmatrix}_{i-1} + \frac{D_{\mathrm{fp}_{j,1}}}{V_{\mathrm{fp}_{j,1}}} \begin{Bmatrix} V_{\mathrm{fp},x_{j,1}} \\ V_{\mathrm{fp},y_{j,1}} \\ V_{\mathrm{fp},z_{j,1}} \end{Bmatrix} + \frac{D_{\mathrm{fp}_{j,0}}}{V_{\mathrm{fp}_{j,0}}} \begin{Bmatrix} V_{\mathrm{fp},x_{j,0}} \\ V_{\mathrm{fp},y_{j,0}} \\ V_{\mathrm{fp},z_{j,0}} \end{Bmatrix} \tag{10}$$

The tether deployment model initially places all tether beads on the lead projectile. As the tether line is payed out, beads are released from the lead projectile into the atmosphere one at a time. A bead is released into the atmosphere when the total mass of the unreeled tether line exceeds the total released bead mass by one bead. When a bead is released into the atmosphere, it is placed along the line from the release point to the last bead released, and initial bead position and velocity conditions are established such that the elastic force across the line is unchanged. This prevents a discontinuity in the line pay-out rate due to bead release. However, because aerodynamic forces act on the bead immediately after it is released, a slight perturbation is generally observed when a bead is released. When a bead is released, the mass of the lead projectile is reduced by the released bead weight, and the length from the release point to the last tether bead released is reset along with the stiffness and damping coefficients of the exiting tether line.

The tether reel is assumed to consist of a rotating reel acted on by the exiting bead elastic force, which tends to pay out the tether line. The reel has a resistance force F_r, which opposes the unreeling process. The equation governing the total length of tether line unreeled is

$$\ddot{s} = \left(F_{T_0} - F_r\right) r^2 / I_r \tag{11}$$

$$I_r = (m_r - ml \cdot s) r^2 / 2 \tag{12}$$

When the full length of tether line has been reached, the acceleration and the velocity of the reel are set to zero. The total amount of tether line released from the reel affects the elastic forces exerted on the tether beads. Although the effective reel radius r decreases as tether line unspools from the reel, this effect is assumed small, and r is set to an average value during a simulation. Expressions for reel resistance as a function of line pay out and line pay-out rate are given by

$$F_r = R_1(\dot{s} - R_2)^2 + 1, \qquad \dot{s} \geq R_2 \tag{13}$$

$$F_r = R_1(s - R_2) + 1, \qquad s \geq R_2 \tag{14}$$

In Eqs. (13) and (14), the constants R_1 and R_2 are design parameters of the reel resistance device.

Determination of Resistance Parameters

To compute the resistance parameters R_1 and R_2, an objective function J is minimized:

$$J = C_1 f_1(T_g) + C_2 f_2(t_{\mathrm{ss}}) + C_3 f_3(T_t) + C_4 f_4(d) \tag{15}$$

In Eq. (15), T_g is the maximum acceleration of the follower projectile, t_{ss} is the time for the system to reach steady state, T_t is the maximum tether line load, d is the maximum deviation of the lead projectile impact point from a nominal trajectory, and C_j are objective function weights. The nominal lead projectile trajectory is defined as the trajectory the lead projectile would follow without a tether reel resistance mechanism employed. The functions f_1, f_2, f_3, and f_4 all take on the form

$$f_i(x) = e^{A_1 x + A_0} \tag{16}$$

where the parameters A_1 and A_2 define the objective function element. The objective function is minimized using a nonlinear simplex method. The advantage of this technique is that it requires only function evaluations.

Results

Simulation results are generated using the dynamic model just described using representative physical parameters. The lead projectile weighs 1962 lbf, whereas the follower projectile weighs 19.62 lbf (1% mass ratio). The initial forward velocity of the munition system is 500 ft/s. The drag coefficient ratio of the follower-to-lead projectile is 2. The tether line has the following properties: length of 1000 ft, weight per length of 0.01 lbf/ft, diameter of 0.0082 ft, stiffness of 62,500 lbf/ft, and damping constant of 0.3. For all simulation results, the tether is discretized into 100 particles. The tether

reel weighs 5 lbf and has a radius of 0.25 ft. The skin-friction drag coefficient of the tether line is 0.007 whereas the flat plate drag coefficient is 1.1. The release altitude of the ordnance is 25,000 ft. In the results to follow, the nominal case is when the reel resistance force is zero, or the lack of a reel resistance mechanism. Because the objective function terms are naturally normalized, all objective function weights are set to unity. The constants A_0 and A_1 contained in the objective function elements are generated to create large values of the objective function if the maximum acceleration of the follower projectile, maximum tether line load, maximum trajectory deviation, or time to reach steady state exceeds 80 g, 800 lbf, 750 ft, or 30 s, respectively. The reel resistance parameters that best reduced the objective function for the LRM device are $R_1 = 1697.26$ and $R_2 = 42.62$ whereas the resistance parameters for the LLM mechanism are $R_1 = 0.2511$ and $R_2 = 314.83$.

Figure 3 plots the range of the lead and follower projectiles. Reel resistance has no significant effect on the range of the projectiles. The speed of the lead projectile is shown in Fig. 4. At the snatch point for the nominal case ($t \cong 6\ s$) the speed of the lead projectile is slightly decreased due to the effect of the snatch load. There are no noticeable effects on the lead projectile's speed for the systems fitted with reel resistance mechanisms. Figure 5 shows the speed of the follower projectile. The nominal configuration shows a rapid increase in speed as the tether line grabs the follower projectile during the snatch condition. The follower projectile rebounds toward the lead projectile so much that the tether line becomes slack. With the tether line slack, the follower projectile's speed decreases to seek its steady-state drop velocity. This oscillation continues until a steady-state condition is reached, where the lead and follower projectiles

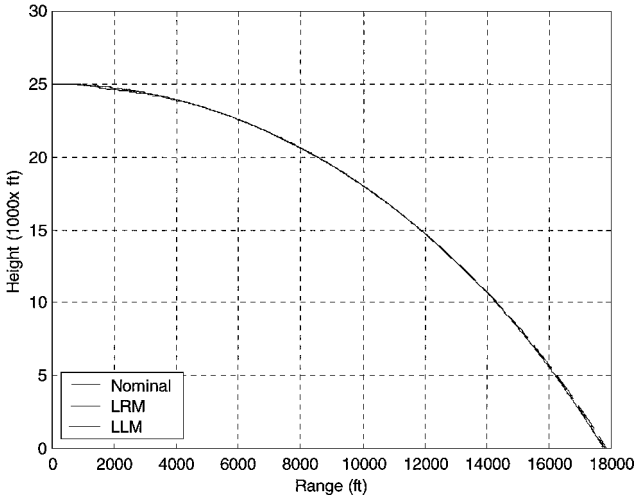

Fig. 3 Range of lead and follower projectiles.

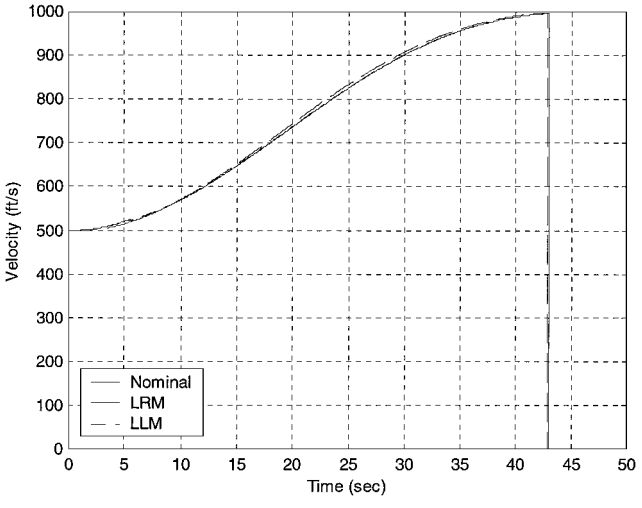

Fig. 4 Speed of lead projectile.

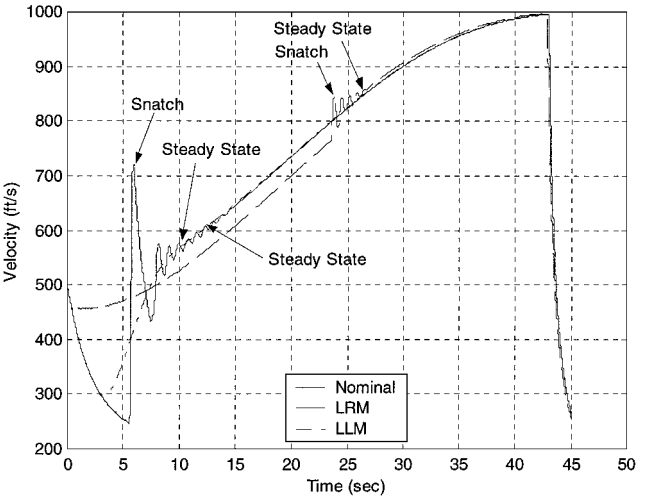

Fig. 5 Speed of follower projectile.

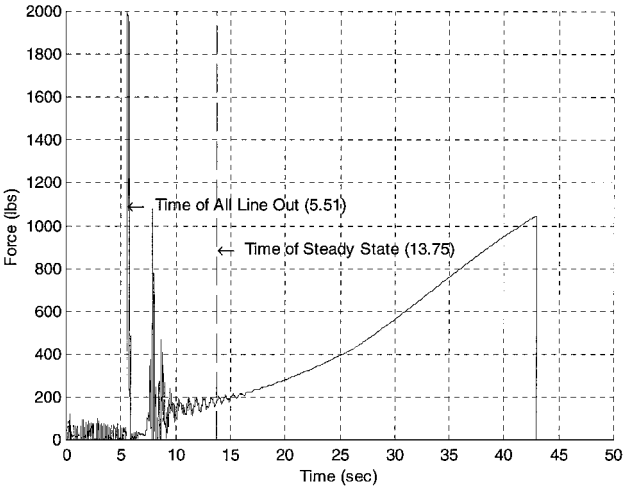

Fig. 6 Tension in the line element adjacent to the follower vs time (nominal).

fall at the same speed. The LRM mechanism drastically reduces the rapid speed changes caused by the snatch condition and consequently the oscillations subside at an accelerated rate. However, the tether line is payed out at a much slower rate, and the snatch condition occurs at approximately 23.5 s into deployment. In this case, a steady-state condition is not achieved until approximately 27.0 s compared to approximately 15.0 s for the nominal case. The LLM device practically eliminates the rapid increase in speed due to the snatch condition, and the oscillations settle at approximately $t = 10.5$ s.

Figures 6–8 show the tension in the line element closest to the follower projectile over the duration of the simulation. Deploying the system with no reel resistance induces a relatively large maximum tether force at snatch. Figure 7 shows that adding the LRM device decreases the snatch load substantially, and Fig. 8 shows that employing the LLM mechanism reduces tension in the tether line element at the snatch point quite dramatically. Note that maximum tension in the tether line is located at different points along the tether line at different time instants during the simulation. The tether line out and line pay out rate as functions of time are shown in Figs. 9 and 10. The LRM device allows the line to accelerate to roughly 42 ft/s and then limits the speed at this value until all of the line is deployed. The LLM mechanism allows the tether line to initially pay out quickly up to a rate of approximately 215 ft/s and then reduces the pay out rate to almost 0 ft/s at the snatch point. The LLM device pays out the tether line at an almost equivalent rate to the nominal case and then drastically slows the rate down just before snatch, which results in greatly reduced snatch loads. The maximum line

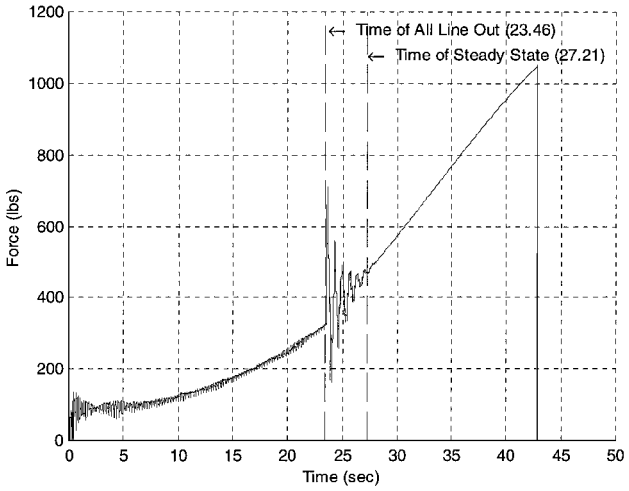

Fig. 7 Tension in the line element adjacent to the follower projectile vs time (LRM).

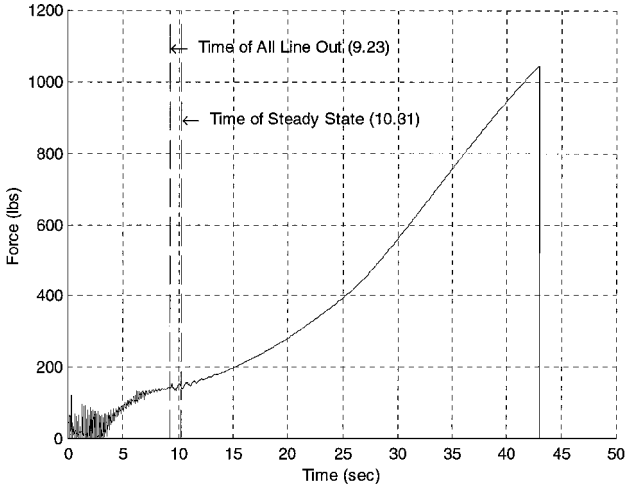

Fig. 8 Tension in the line element adjacent to the follower vs time (LLM).

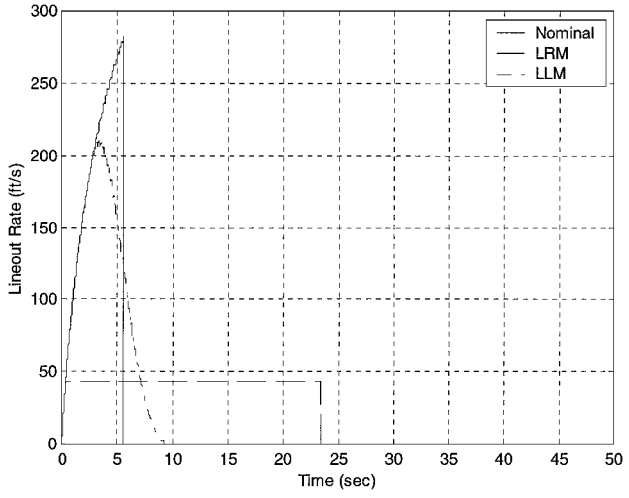

Fig. 9 Tether line pay-out rate.

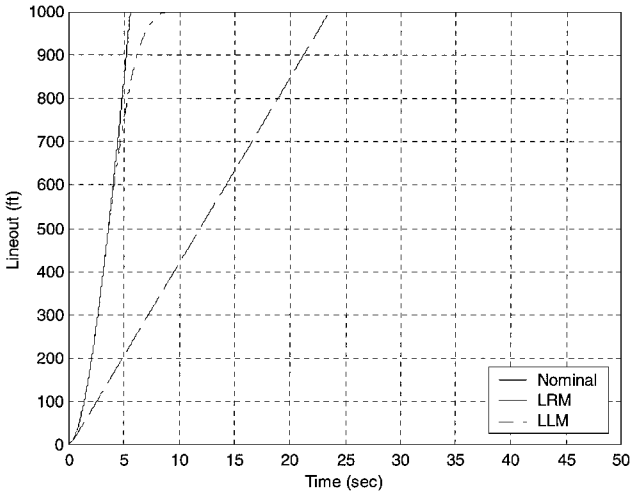

Fig. 10 Tether line pay out.

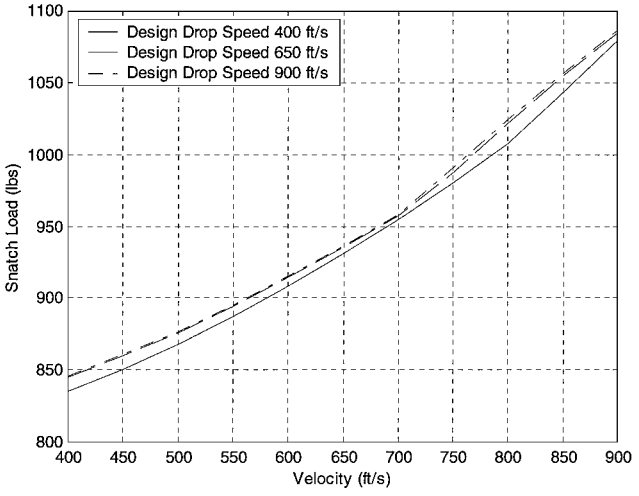

Fig. 11 Maximum snatch load vs forward drop speed (LRM).

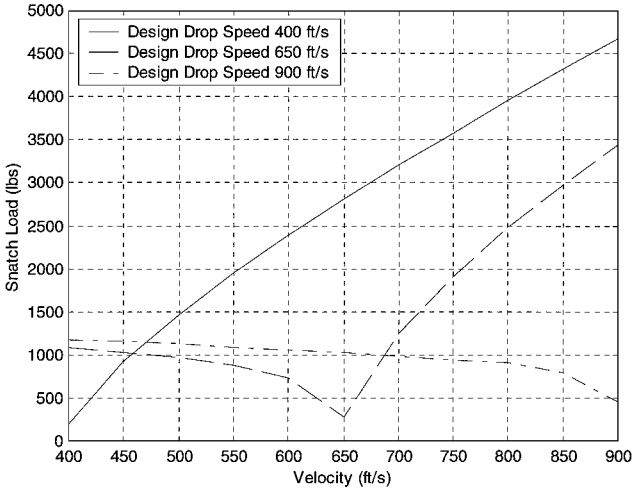

Fig. 12 Maximum snatch load vs forward drop speed (LLM).

loads at snatch occur in the tether line element adjacent to the lead projectile and are 2304, 880, and 189 lbf for the nominal, LRM, and LLM mechanisms. It is apparent that adding a reel resistance mechanism significantly reduces the snatch loads from that of a system with no reel resistance. The maximum acceleration of the follower projectile is 89.4, 17.5, and 5.6 g for the nominal, LRM, and LLM cases. This reduction in acceleration of the follower projectile creates a safeguarded platform for sensors. The time for the follower projectile to reach steady state is 13.6, 27.2, and 10.3 s for the nominal, LRM, and LLM mechanisms. The LRM mechanism serves to increase the time it takes the system to reach a steady-state condition as compared with the nominal case by more than 13 s. The LLM device, on the other hand, decreases the acceleration of the follower and the tension in the tether line at snatch, but it also decreases the time to reach steady state by roughly 3.3 s.

Figures 11–22 show how system performance changes when a reel resistance mechanism that is designed for a specific point is

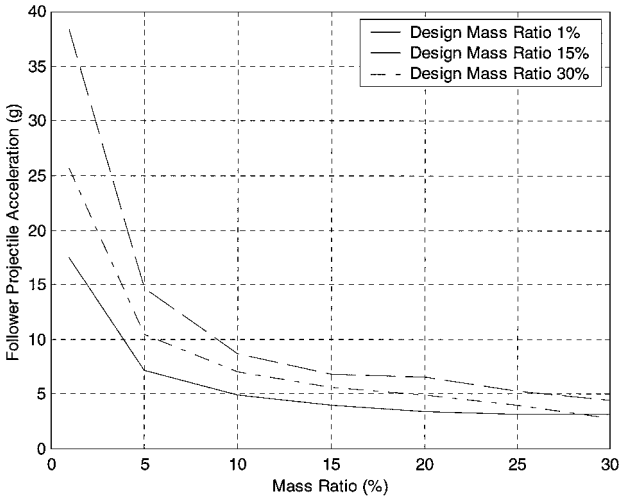

Fig. 13 Maximum acceleration of follower projectile vs mass ratio (LRM).

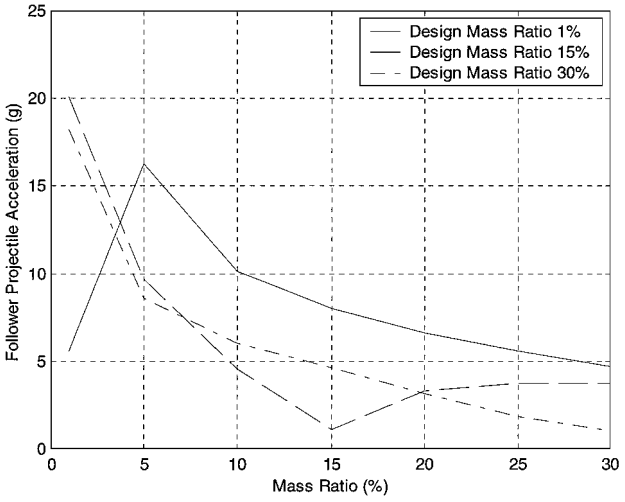

Fig. 14 Maximum acceleration of follower projectile vs mass ratio (LLM).

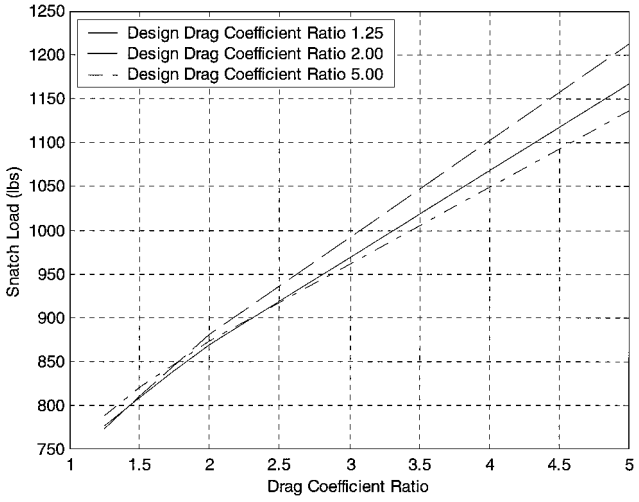

Fig. 15 Maximum snatch load vs drag coefficient ratio (LRM).

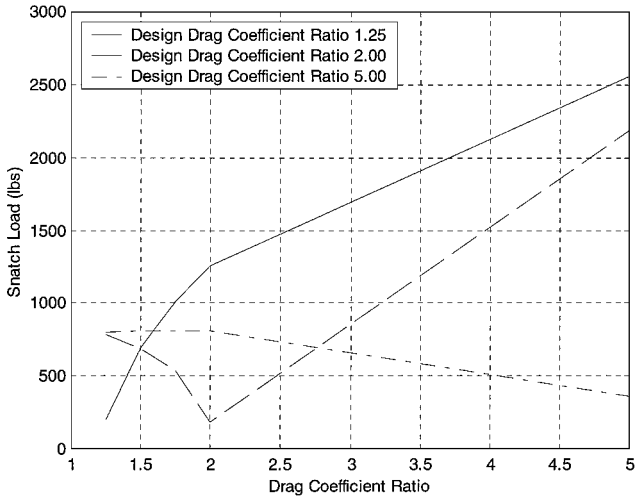

Fig. 16 Maximum snatch load vs drag coefficient ratio (LLM).

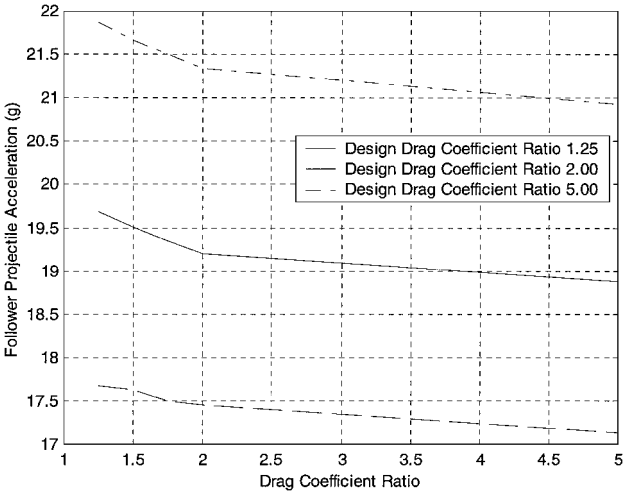

Fig. 17 Maximum acceleration of follower projectile vs drag coefficient ratio (LRM).

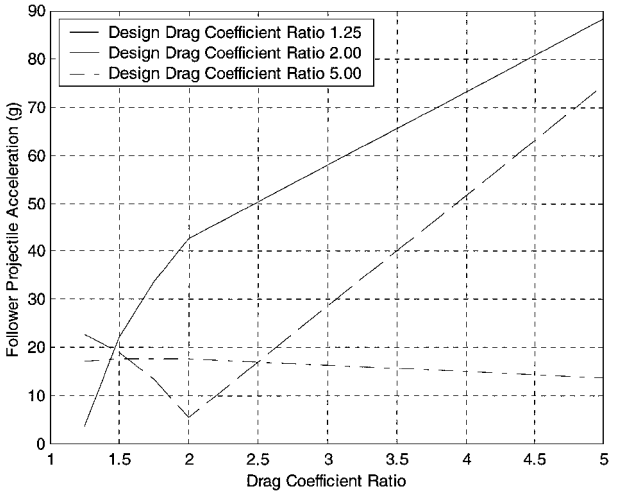

Fig. 18 Maximum acceleration of follower projectile vs drag coefficient ratio (LLM).

employed under off-design conditions. Reel resistance mechanisms tailored to specific drop speeds, projectile mass ratios, projectile drag coefficient ratios, and tether stiffness are considered. Figures 11 and 12 show the maximum snatch loads generated for LRM and LLM devices designed for 400-, 650-, and 900-ft/s drop speeds. At each design drop velocity, the LRM and LLM resistance functions are generated by minimizing the objective function discussed earlier. Figures 11 and 12 present how off-design drop speeds effect the resistance device performance. For the LRM mechanism, the snatch force steadily increases with drop speed. The LLM mechanism produces local regions of reduced snatch loads associated with the design condition.

As shown in Figs. 13 and 14, the follower projectile maximum acceleration decreases as a function of the mass ratio for the LRM mechanism. Mass ratio is defined as the mass of the follower projectile divided by the mass of the lead projectile. The mechanism

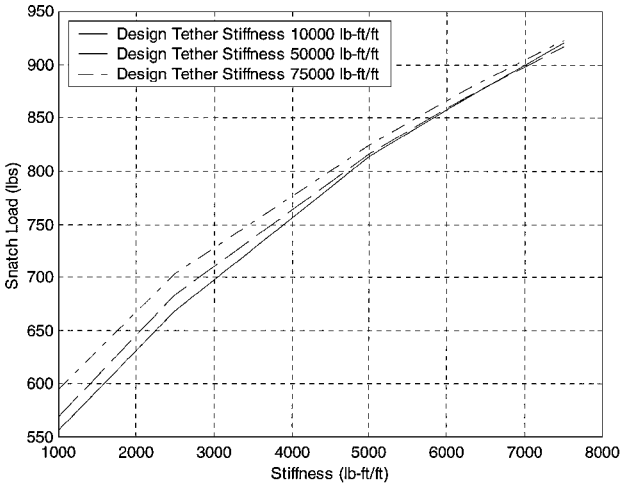

Fig. 19 Maximum snatch load vs tether stiffness (LRM).

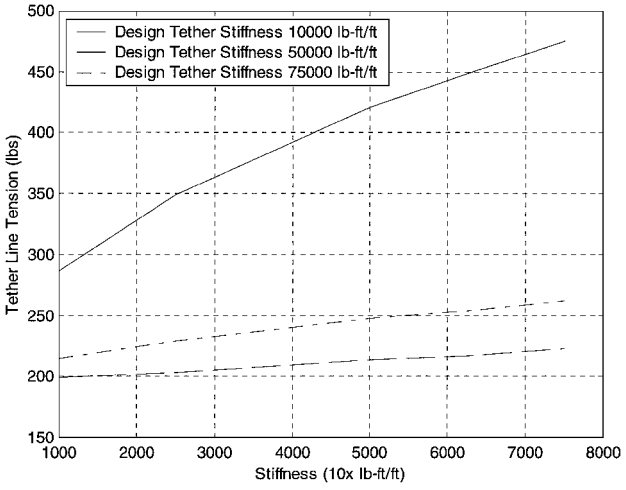

Fig. 20 Maximum snatch load vs tether stiffness (LLM).

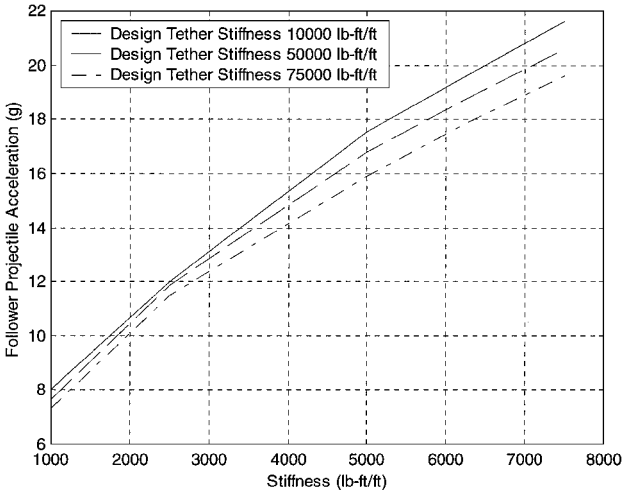

Fig. 21 Maximum acceleration of follower projectile vs tether stiffness (LRM).

designed for low mass ratio performs best. On the other hand, the LLM mechanisms perform best in a local area near their design point. As the mass of the follower increases, its steady-state drop speed becomes closer to that of the lead projectile, and consequently the separation time increases. Because the LRM device is only effective at limiting the speed at which the line is paid out, it is not capable of decreasing the separation time of the two projectiles. It actually works to increase the time to reach steady state for the larger

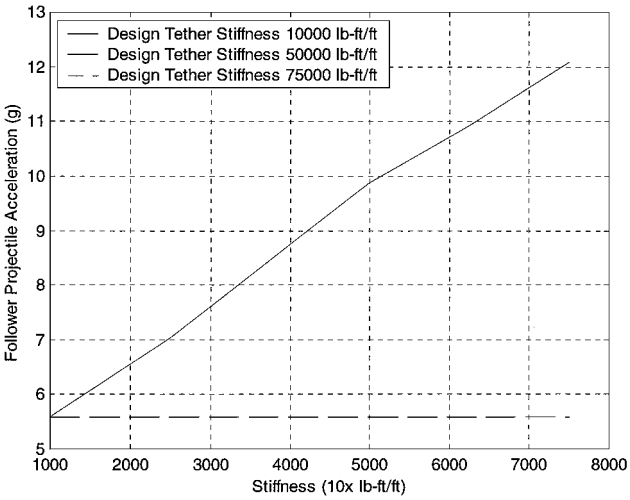

Fig. 22 Maximum acceleration of follower projectile vs tether stiffness (LLM).

mass ratios. The LLM mechanism can pay out tether line at a rapid rate and then reduce the speed of the exiting line as it approaches snatch.

The drag coefficient ratio is defined as the drag coefficient of the follower projectile divided by the drag coefficient of the lead projectile. For the LRM device, as the drag coefficient ratio increases, rapid increases in tether line loads similar to snatch loads are produced before all of the tether line is deployed. These loads are a result of the follower projectile separating from the lead projectile at an increased rate due to aerodynamic drag and then being brought to a halt by the line out rate-limiting action of the reel resistance. In Fig. 15 it can be seen that the maximum snatch load for the LLM device steadily increases with increased drag ratio. Figure 16 shows that because the LLM mechanism allows the tether line to pay out at a rapid rate and then gradually reduces this rate to approximately zero at snatch, the maximum tether line load can be greatly reduced for a mechanism designed for a particular drag coefficient ratio. A function optimized around a drag coefficient ratio of 2 is also effectual in limiting the snatch loads up to drag coefficient ratios as high as 3.25.

Figure 17 plots the maximum acceleration of the follower projectile as a function of drag coefficient ratio for the LRM mechanism. Because the speed of separation is limited, the follower projectile acceleration is a result of the initial separation of the projectiles and not a result of the snatch condition. The maximum acceleration of the follower projectile slightly decreases with increasing drag coefficient ratio. In Fig. 18, the acceleration of the follower projectile is plotted as a function of the drag coefficient ratio for the LLM device. In this case, follower projectile acceleration for the reel designed for a drag coefficient ratio of 1.25 grows in magnitude because the reel resistance proportional to line out can not create sufficient resistance to limit the tether line out rate for the higher drag coefficient ratios. For the reel designed for a drag coefficient ratio of 2.00, the follower projectile maximum acceleration is greater in magnitude for lower drag coefficient ratios because the resistance becomes too great and a rapid growth in tether line load is induced before all of the tether line is deployed. The reel designed for a drag coefficient ratio of 5.00 produces sufficient resistance to limit the line out rate through the entire simulation, which produces lower follower projectile acceleration at the snatch point. However, the time to reach steady state is increased because the time for all of the tether line to pay out is increased due to the reel resistance.

Figures 19–22 show that maximum tether line loads and maximum follower projectile acceleration are directly proportional to tether stiffness, independent of the reel resistance mechanism employed. This demonstrates that, to reduce snatch loads and follower accelerations and to maintain an acceptable time to reach steady state, lessened tether stiffness along with a reel resistance mechanism should be employed.

Conclusions

Two load-limiting mechanisms were examined to alleviate the problem of exceedingly high tether line loads and follower projectile acceleration when it is fully unreeled by two projectiles falling in the atmosphere. The LRM mechanism forces the tether line to unspool at a constant rate. Because the unspooling rate is limited, the tether line requires a significantly longer time to fully deploy. Furthermore, although the snatch load is reduced with respect to a system with no reel resistance, a notable snatch load is still present because of the abrupt change in tether line pay out rate when the tether line is fully deployed. Thus, a fundamental trade exists between the time to deploy fully the tether line and the maximum tether line load. Relative to the LLM mechanism, the LRM mechanism can be utilized over a wide drop speed range and should be designed for the highest design drop speed. The LLM mechanism produces a large line out rate initially, which releases the bulk of the line. When the line is nearly fully deployed, the reel resistance is increased to reduce the tether line out rate, which in turn reduces the maximum tether line loads. Thus, the LLM mechanism has the advantage of quickly deploying the tether while dramatically reducing maximum tether line loads and follower projectile acceleration. The main drawback of the LLM mechanism is that it must be tuned to a specific drop speed. An LLM mechanism that is designed for a particular drop speed, projectile mass ratio, or projectile drag ratio does not perform well under conditions away from the design point. Hence, for systems with a tightly controlled operational environment, the LLM device performs best, but for systems that operate under significantly varying operational conditions, the LRM unreeling mechanism is superior.

References

[1]Tye, G., and Han, R., "Attitude Dynamics Investigation of the OEDIPUS—A Tethered Rocket Payload," *Journal of Spacecraft and Rockets*, Vol. 32, No. 1, 1995, pp. 133–141.

[2]Puig-Suari, J., Longuski, J., and Tragesser, S., "Aerocapture with a Flexible Tether," *Journal of Guidance, Control, and Dynamics*, Vol. 18, No. 6, 1995, pp. 1305–1312.

[3]No, T. S., and Cochran, J. E., "Dynamics and Control of a Tethered Flight Vehicle," *Journal of Guidance, Control, and Dynamics*, Vol. 18, No. 1, 1995, pp. 2411–2429.

[4]Clifton, J. M., Schmidt, L. V., and Stuart, T. D., "Dynamic Modeling of a Trailing Wire Towed by an Orbiting Aircraft," *Journal of Guidance, Control, and Dynamics*, Vol. 18, No. 4, 1995, pp. 875–881.

[5]Doyle, G. R., Jr., "Mathematical Model for the Ascent and Descent of a High-Altitude Tethered Balloon," *Journal of Aircraft*, Vol. 6, No. 5, 1969, pp. 457–462.

[6]Matthews, W., "Camera May Relay Instant Images of Bomb Damage," *Airforce Times*, Vol. 58, No. 1, 1997, p. 30.

[7]Djerassi, S., and Bamberger, H., "Simultaneous Deployment of a Cable from Two Moving Platforms," *Journal of Guidance, Control, and Dynamics*, Vol. 21, No. 2, 1998, pp. 271–276.

[8]Costello, M., and Frost, G., "Simulation of Two Projectiles Connected by a Flexible Tether," *Proceedings of the AIAA Atmospheric Flight Mechanics Conference and Exhibit*, AIAA, Reston, VA, 1998, pp. 360–369.

[9]Von Mises, R., *Theory of Flight*, Dover, New York, 1959, pp. 8–13.